The FEBS Journal

FEBS PRESS science publishing by scientists

RAGE induces physiological activation of NADPH oxidase in neurons and astrocytes and neuroprotection

Evgenia S. Seryogina[1], Anna V. Kamynina[2,3], Dmitry O. Koroev[3], Olga M. Volpina[3], Andrey Y. Vinokurov[1] and Andrey Y. Abramov[1,4]

1 Orel State University, Russia
2 Research Center for Molecular Mechanisms of Aging and Age-Related Diseases, Moscow Institute of Physics and Technology (National Research University), Dolgoprudny, Russia
3 Shemyakin-Ovchinnikov Institute of Bioorganic Chemistry, Russian Academy of Sciences, Moscow, Russia
4 Department of Clinical and Movement Neurosciences, UCL Queen Square Institute of Neurology, London, UK

Keywords
astrocytes; NADPH oxidase; neurons; RAGE; reactive oxygen species; β-amyloid

Correspondence
A. Y. Abramov, UCL Queen Square Institute of Neurology, London WC1N 3BG, UK
Tel: +44 2034484062
E-mail: a.abramov@ucl.ac.uk

Evgenia S. Seryogina and Anna V. Kamynina contributed equally to this work.

(Received 7 September 2023, revised 8 January 2024, accepted 30 January 2024)

doi:10.1111/febs.17086

The transmembrane receptor for advanced glycation end products (RAGE) is a signaling receptor for many damage- and pathogen-associated molecules. Activation of RAGE is associated with inflammation and an increase in reactive oxygen species (ROS) production. Although several sources of ROS have been previously suggested, how RAGE induces ROS production is still unclear, considering the multiple targets of pathogen-associated molecules. Here, using acute brain slices and primary co-culture of cortical neurons and astrocytes, we investigated the effects of a range of synthetic peptides corresponding to the fragments of the RAGE V-domain on redox signaling. We found that the synthetic fragment (60–76) of the RAGE V-domain induces activation of ROS production in astrocytes and neurons from the primary co-culture and acute brain slices. This effect occurred through activation of RAGE and could be blocked by a RAGE inhibitor. Activation of RAGE by the synthetic fragment stimulates ROS production in NADPH oxidase (NOX). This RAGE-induced NOX activation produced only minor decreases in glutathione levels and increased the rate of lipid peroxidation, although it also reduced basal and β-amyloid induced cell death in neurons and astrocytes. Thus, specific activation of RAGE induces redox signaling through NOX, which can be a part of a cell protective mechanism.

Introduction

The transmembrane receptor for advanced glycation end products (RAGE) is a multiligand receptor able to bind number of abnormal peptides and proteins, including advanced glycation end-products (AGEs) which gave the name of the receptor, amphoterin, calgranulins and amyloid-beta (Aβ) peptides. Expression of the RAGE is shown in many tissues and cells, including neurons and astrocytes [1]. Although RAGE activation is considered to be involved in the onset and progression of proinflammatory or proapoptotic cell responses [2], the role of RAGE in physiological processes such as cell differentiation, glutamate release and calcium signaling has been demonstrated [3,4].

Redox signaling is based on the activation of the redox reactions and production of the reactive oxygen species (ROS) for signaling purposes in various

Abbreviations
Aβ, β-amyloid; DPI, diphenyleneiodonium chloride; GSH, glutathione; HBSS, Hanks' balanced salt solution (HBSS); HEt, dihydroethidium; MCB, monochlorobimane; NOX, NADPH oxidase; PI, propidium iodide; RAGE, receptor for advanced glycation end products; ROS, reactive oxygen species.

enzymes of the cells [5]. Changes in the balance between production of ROS and efficiency of antioxidant system in brain cells can be a trigger for pathology and cell death that also can possibly be regulated by intracellular signaling [6]. One of the major producers of ROS in the brain cells, NADPH oxidase, is involved in processes of physiology and pathology [7–9]. Although activation of NADPH oxidase (NOX) in different cells is shown through receptor dependent and receptor independent pathways, as a result of involvement in phagocytic processes, it can be activated by abnormal peptides and proteins, including Aβ [8,10]. RAGE was shown to be able to increase expression of the major NOX isoforms in the brain: NOX2, NOX 4 and NOX1 [11–13]. However, it can work in an opposite direction and inhibitors of NOX reduce RAGE expression [14]. Most of the RAGE activators that are used as RAGE agonists, including Aβ, have multiple targets and it is difficult to separate the activity of these peptides or molecules on RAGE from other effects.

Recently, we used a range of synthetic peptides corresponding to the fragments of the RAGE V-domain in various experiments and have found that the synthetic fragment of V-domain (60–76) protects the memory of bulbectomized and transgenic mice exhibiting major features of Alzheimer's disease, penetrating into the mouse brain [15,16]. Moreover, in *in vitro* experiments, it also activates glutamate release from astrocytes and induces calcium signal in neurons [4] and protects neurons against Aβ induced apoptosis [17]. Considering that all the *in vitro* effects of the synthetic fragment (60–76) were dependent on the RAGE inhibitor, we suggested that this RAGE peptide (60–76) could possibly interact with the same domain of the RAGE receptor. In the present study, we also used the short fragments of peptide (60–76) and the protected analogue of the RAGE peptide (60–76), which was previously discovered to demonstrate a more prolonged effect on the state of the memory of bulbectomized and transgenic mice compared to the free peptide (60–76) [16,18].

Here, we investigated the effect of the RAGE peptides on the reactive oxygen species production in primary neurons and astrocytes and acute brain slices. We have found that only the RAGE peptides (60–76) and Ac-(60–76)-NH_2 induce ROS production in neurons and astrocytes via the RAGE-dependent activation of NOX, but not its short fragments. This activation of NOX did not induce oxidative stress and cell death. Thus, RAGE activation plays important role in redox signaling through activation of NOX.

Results

Two RAGE peptides induce activation of ROS production in acute brain slices

Because of the complexity of brain bioenergetics based on complicated intercellular neuron–glia interaction, acute brain slices appear to be the most relevant model for the research of receptor-linked processes [19]. ROS production rate was assessed using dihydroethidium (HEt), which transforms to fluorescent ethidium with exciting at 530 nm after oxidation by mainly superoxide anion. For detecting the possibility of activating ROS production, six RAGE peptides solutions (10 μM) were added after recording the basal increase in ethidium fluorescence (Fig. 1A–F). The degree of peptides-based ROS production activation was calculated as a percentage of the basal level (Fig. 1G). As can be seen, RAGE peptides (60–76) (P1) and Ac-(60–76)-NH_2 (P7) are characterized by the significant increase in HEt oxidation rate (221 ± 76%, $n = 3$ slices, $P = 0.002$ and 487 ± 55%, $n = 3$ slices, $P = 0.001$ respectively) compared to other peptides P2–P5.

Two RAGE peptides induce activation of ROS production in primary co-cultures of neurons and glial cells

Determination of the ROS production source that can be activated by the RAGE peptides requires a complex of *in vitro* experiments with a number of selective inhibitors. Yo ensure that stimulation effect of peptides identified *ex vivo* can be registered in a cell culture, we assessed the HEt oxidation process in the presence of RAGE peptides in primary co-cultures of cortical neurons and glial cells (Fig. 2A–F). In full compliance with the data presented above, P1 and P7 demonstrate 1.7-fold ($P < 0.001$) and 1.8-fold ($P < 0.001$) activation of ROS production, whereas no significant change in HEt oxidation rate was registered in the case of the other fragments (Fig. 2I). Consequently,

Fig. 1. RAGE peptides activate ROS production in cortical acute slices. (A–F) Representative traces of HEt fluorescence intensity from singe cells increase before and after the addition of peptides (10 μM). (G) Quantification of the changes in HEt oxidation rate after peptide addition (data are shown as a percentage of the basal level of HEt fluorescence increase rate before peptide addition). Arrows in the traces continue the basal rate of HEt fluorescence. Data are presented as the mean ± SEM.

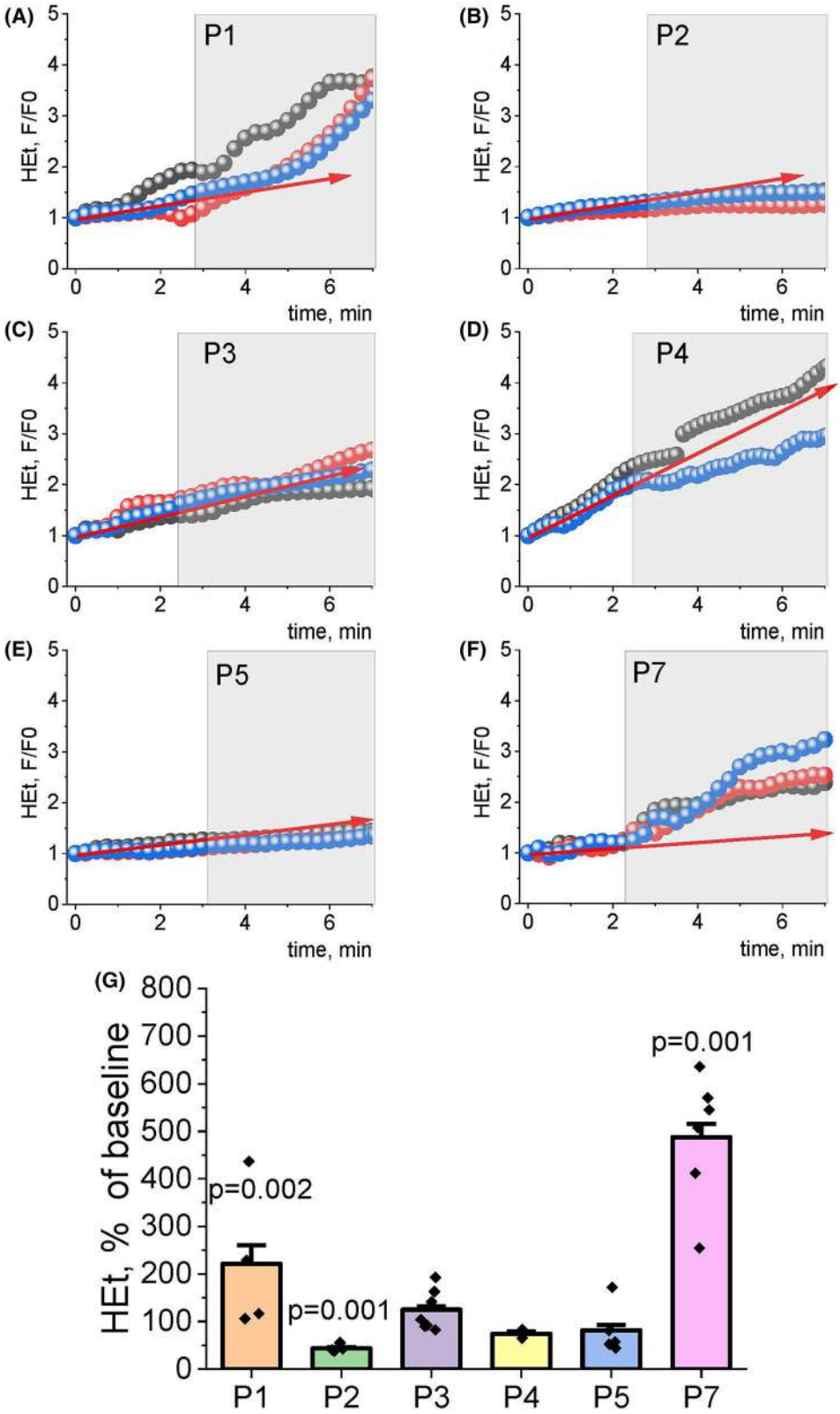
(A)
P1
HEt, F/F0
time, min
(B)
P2
HEt, F/F0
time, min
(C)
P3
HEt, F/F0
time, min
(D)
P4
HEt, F/F0
time, min
(E)
P5
HEt, F/F0
time, min
(F)
P7
HEt, F/F0
time, min
(G)
HEt, % of baseline
p=0.002
p=0.001
p=0.001
P1
P2
P3
P4
P5
P7

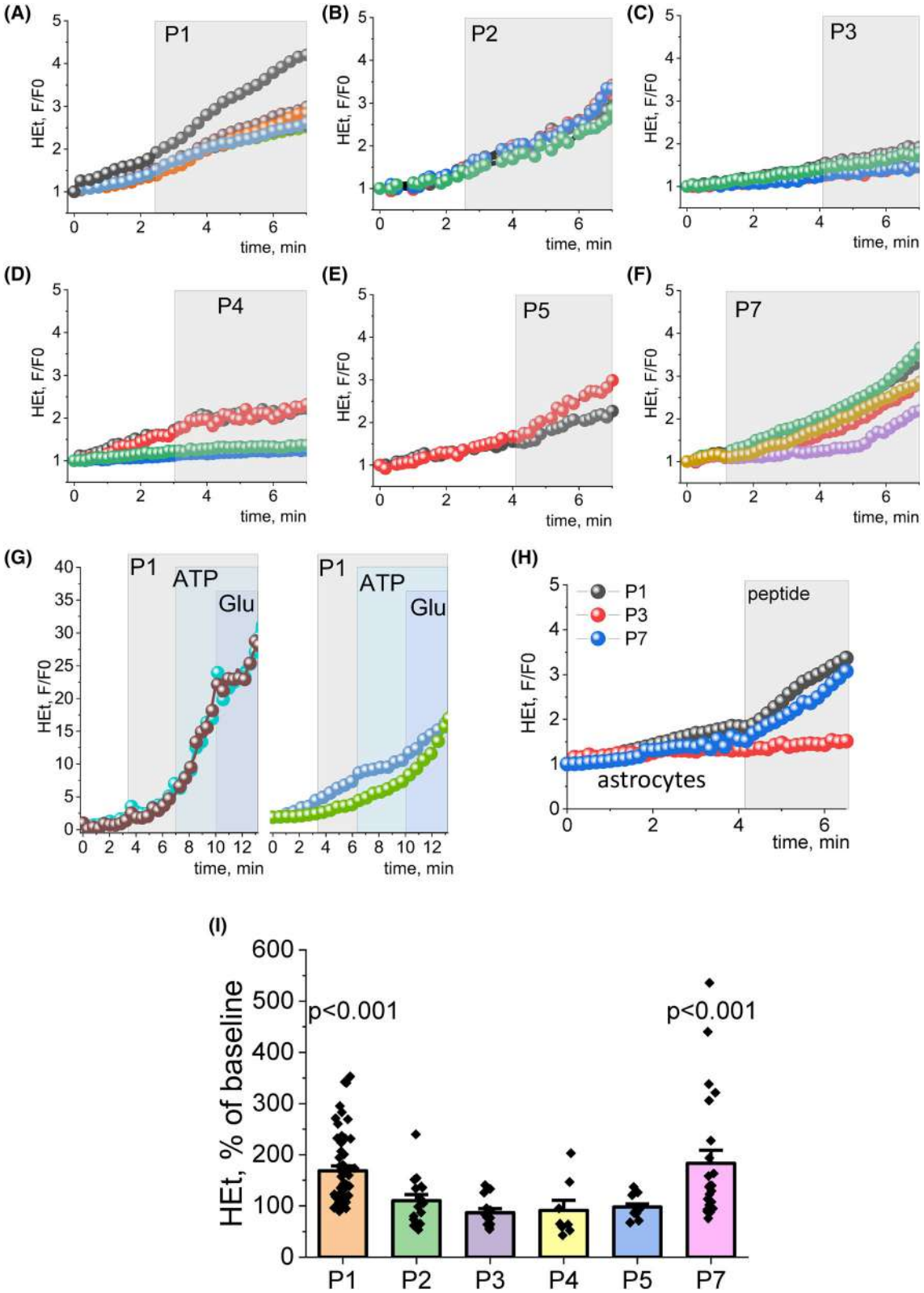

Fig. 2. Activation of ROS production in cortical neurons and astrocytes by RAGE peptides P1 and P7 *in vitro*. (A–F) Representative traces of HEt fluorescence intensity increase before and after peptide addition (10 μM). (G) Application of the 100 μM ATP and 10 μM glutamate for activation of ROS production and identification of the astrocytes and neurons in cortical co-culture. (H) Effect of peptide fragments P1, P3 and P7 on the rate of Het fluorescence in pure primary culture of astrocytes. (I) Quantification of the changes in HEt oxidation rate after peptide addition (data are shown as a percentage of the basal level of HEt fluorescence increase rate before peptide addition). Each line corresponds to a single cell. Data are presented as the mean ± SEM.

the two most active peptides, P1 and P7, were chosen for further research. Non-active short peptide P3 was used as a negative control peptide.

Neurons and astrocytes could be activated by specific neurotransmitters and gliotransmitters that specifically induce ROS production in these cells [20,21]. It should be noted that P1 induced activation of ROS production in both neurons and astrocytes. Neuronal activation was confirmed by the selective response of these cells to 10 μM glutamate (Fig. 2G) and astrocytic signal by activation of these cells with 100 μM ATP (Fig. 2G). The stimulating effect of P1and P7 but not short peptide P3 on the rate of ROS production on glia cells was also confirmed in the experiments with a pure primary culture of astrocytes (Fig. 2H).

RAGE fragment-induced increase in ROS production is mediated by NOX activation

Among the ROS intracellular sources, activation of NOX or xanthine oxidase appears to be the most probable reason for peptide fragment-based stimulation of HEt oxidation in cytosol. To determine the role of these enzymes in redox balance change after the influence of RAGE peptide fragments, primary co-cultures of cortical neurons and glial cells were incubated for 30 min with the NOX inhibitor, diphenyleneiodonium chloride (DPI) (0.5 μM) and xanthine oxidase inhibitor oxypurinol (20 μM) before the experiments with HEt oxidation (Fig. 3A–D). Calculations performed show no increase in ROS production in the presence of DPI in the case of peptides P1 and P7, as well as control P3, and after the influence of phorbol 12-myristate 13-acetate, a protein kinase C activator. At the same time, inhibition of xanthine oxidase by oxypurinol did not have any effect on the ability of RAGE peptide (60–76) (P1) or P7 with respec to activating the ethidium fluorescence growth rate (Fig. 3E).

Peptides (60–76) and Ac-(60–76)-NH_2 increase ROS production through direct RAGE activation

NOX-based increase in ROS production after influence of RAGE peptides may be the result of direct RAGE activation or be mediated by the other intracellular signal pathways. Pre-incubation of the cells with the selective antagonist, blocker of RAGE V domain-mediated ligand binding, FPS-ZM1 (1 μM) (Fig. 4A–C), effectively blocked the increase in ROS production induced by peptides P1 and P7 (Fig. 4D) and had no influence on the stimulation effect of phorbol 12-myristate 13-acetate (Fig. 4A). Previously, we have shown that P1 can activate glutamate receptors in neurons that also can activate NOX [4]. Pre-incubation (20 min) of the neurons and astrocytes with CNQX (10 μM) and MK-801 (10 μM), AMPA/kainate and NMDA receptor inhibitors did not change the effect of RAGE activation on NOX and application of P1 led to a two-fold ($n = 3$ coverslips, $N = 39$ cells, $P < 0.001$) and four-fold ($n = 3$ coverslips, $N = 16$ cells, $P < 0.001$) increase in the HEt oxidation rate in the presence of AMPA/kainate, as well as NMDA receptors inhibitors, respectively (Fig. 4E–G). It should be noted that both CNQX or MK-801 had no effect on the P7-induced increase in ROS production in neurons and astrocytes (Fig. 4G).

Activation of RAGE induces ROS production but not oxidative stress

To detect possible changes in redox balance after RAGE activation by peptide, we unraveled the effect of the peptides on the level of glutathione (GSH) (Fig. 5A–E) and lipid peroxidation rate (Fig. 5F–M). Two hours of incubation of primary co-culture of cortical astrocytes and neurons with P1 led to a minor decrease in GSH content (73.7 ± 0.7% of control cells, $n = 3$ coverslips, $N = 2800$ cells, $P < 0.0001$) (Fig. 5E) and an increase in lipid peroxidation rate (187 ± 23% of basal level, $n = 3$ coverslips, $N = 27$ cells, $P = 0.01$) (Fig. 5F,L), which also can be blocked by DPI (Fig. 5I,M). P3 and P7 show no decrease in GSH content (Fig. 5E) and no acceleration of lipid peroxidation (Fig. 5G,H,L). However, minor changes in GSH and lipid peroxidation level by P1 and no changes by P7 are not indicative of the development of oxidative stress leading to cell death.

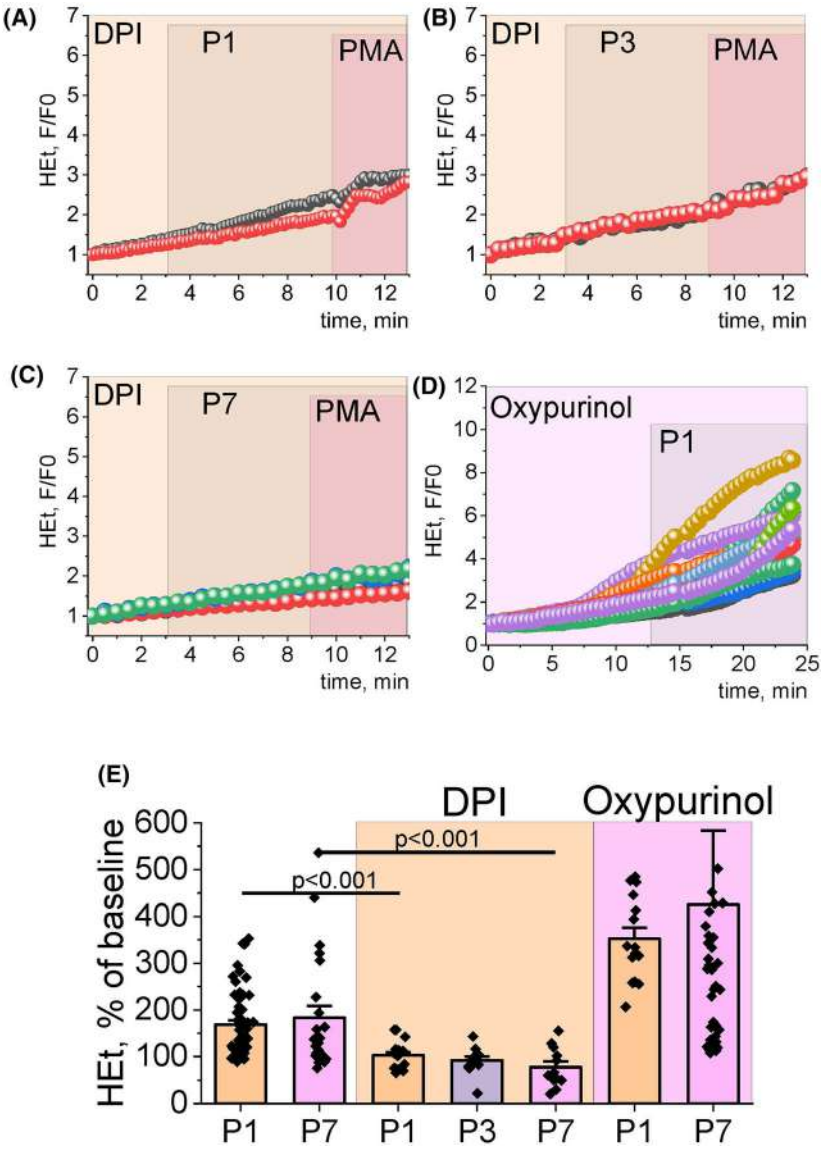

Fig. 3. RAGE peptides P1 and P7 induce NOX activation. Inhibition of NOX by DPI (0.5 μM) eliminates the activation of ROS production following the addition of 10 μM P1 (A), P7 (C) and control P3 (B). Application of the xanthine oxidase inhibitor, oxypurinol (20 μM), has no effect on the stimulation of HEt oxidation by P1 (D). (E) Quantification of the effects of NOX and xanthine oxidase inhibitors on the changes in HEt oxidation rate after the addition of peptides P1, P3, and P7 (data are shown as a percentage of the basal level of HEt fluorescence increase rate before peptide addition). Each line corresponds to a single cell. Data are presented as the mean ± SEM.

RAGE activation does not induce cell death in primary neuroglial co-cultures

Incubation of primary co-cultures of cortical neurons and glial cells with P1 did not increase the percentage of propidium iodide (PI)-positive cells (8.0 ± 1.4%, $n = 3$ coverslips, $N = 21$ fields of view) compared to cells without any exposure (12.8 ± 1.7%, $n = 3$ coverslips, $N = 47$ fields of view) (Fig. 6). The dead cells level in P7-treated culture was higher than in the control experiment (19.3 ± 2.6%, $n = 3$ coverslips, $N = 31$ fields of view, $P = 0.003$) but equal to that in the culture incubated with P3 (19.6 ± 2.6%, $n = 3$ coverslips,

Fig. 4. The increase in ROS production in brain cells after application of P1 and P7 is mediated by specific activation of RAGE. Incubation of primary co-culture of cortical astrocytes and neurons with a RAGE antagonist suppressed the activation of HEt oxidation rate by peptide P1 (A) and peptide P7 (C) and did not impact the effect of control peptide P3 (B). ROS production after incubation with FPS-ZM1 (1 μM) and P1, P3 or P7 was comparable to the baseline level taken as 100% (D). Blocking AMPA receptors (E) and NMDA receptors (F) by pre-incubation with CNQX (10 μM) and MK-801 (10 μM), respectively, does not suppress the increase in HEt oxidation rate after treatment with P1. (G) The peptide-based increase in ROS production rate is shown after incubation with NMDA receptor and AMPA receptor antagonists (data are shown as a percentage of the basal level of HEt fluorescence increase rate before peptide addition). Each line corresponds to a single cell. Data are presented as the mean ± SEM.

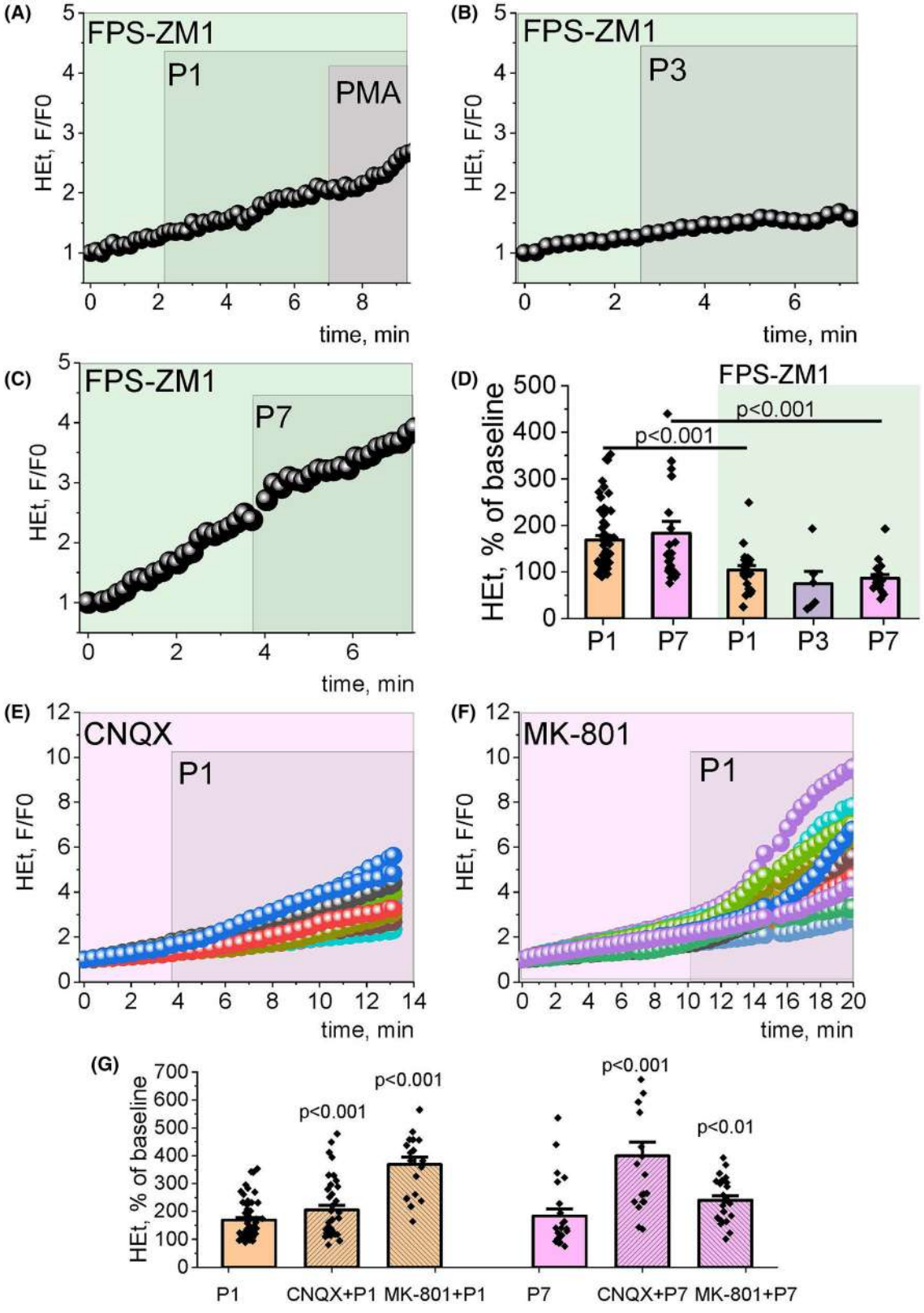
(A)
FPS-ZM1
P1
PMA
HEt, F/F0
time, min
(B)
FPS-ZM1
P3
HEt, F/F0
time, min
(C)
FPS-ZM1
P7
HEt, F/F0
time, min
(D)
FPS-ZM1
HEt, % of baseline
p<0.001
p<0.001
P1
P7
P1
P3
P7
(E)
CNQX
P1
HEt, F/F0
time, min
(F)
MK-801
P1
HEt, F/F0
time, min
(G)
HEt, % of baseline
p<0.001
p<0.001
p<0.001
p<0.01
P1
CNQX+P1
MK-801+P1
P7
CNQX+P7
MK-801+P7

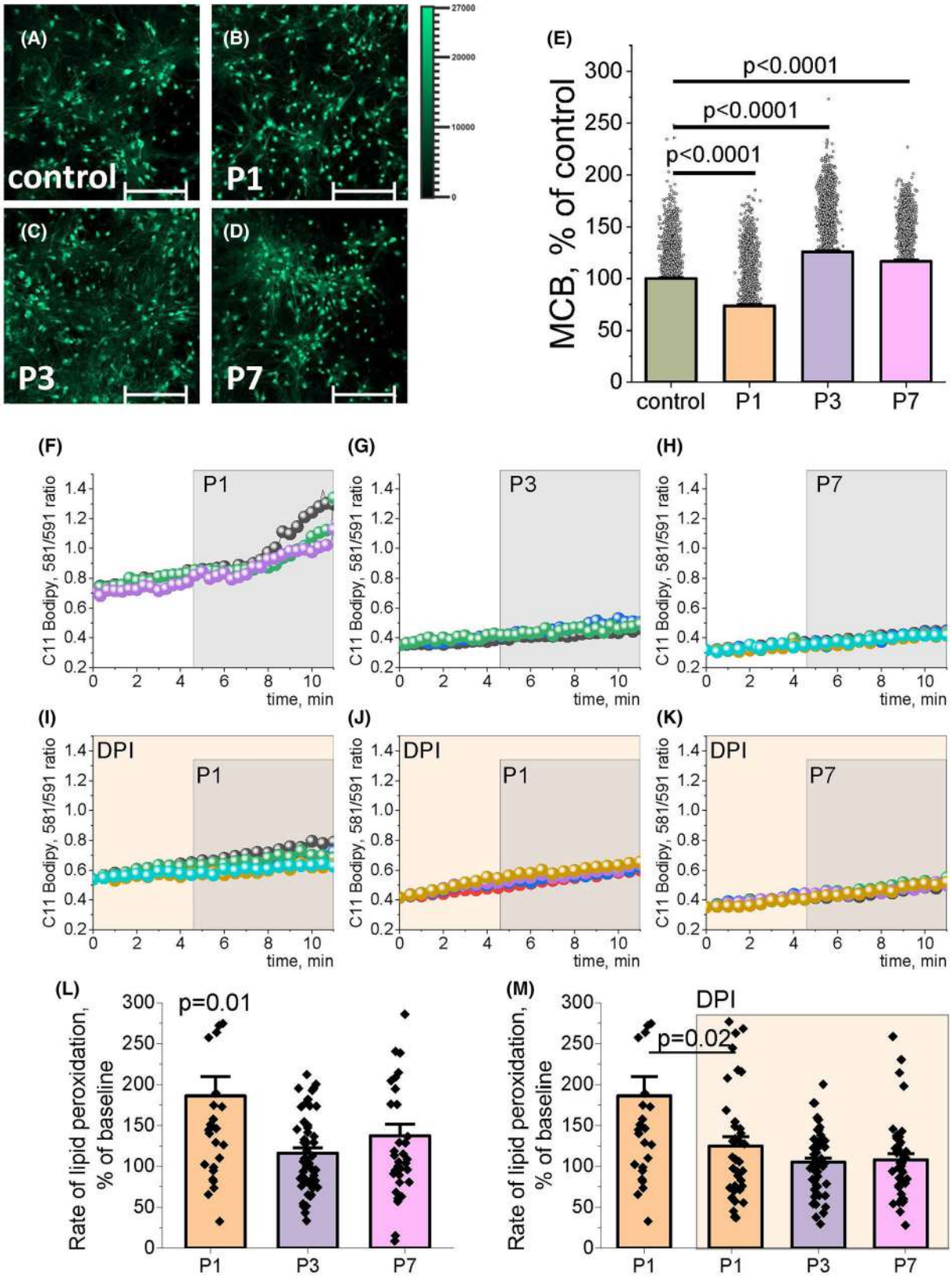

Fig. 5. Activation of RAGE leads to a decrease in GSH levels and increases the rate of lipid peroxidation in cortical cells. Representative confocal images of MCB-loaded primary co-culture of cortical astrocytes and neurons without any exposure (A) (control) and after preincubation with peptide P1 (B), P3 (C) and P7 (D). Scale bar = 200 μm. (E) Fluorescence intensity of MCB in cortical cells after pre-incubation with peptides, normalized to the level of control group cells without incubation. Changes in the oxidation rate of C-11 BODIPY 581/591 after addition of P1, P3 and P7 only (F–H, L) and after pre-incubation with NOX inhibitor DPI (0.5 μM) (I, J, K, M). Data were normalized to the basal level of lipid peroxidation rate taken as 100%. Each line corresponds to a single cell. Data are presented as the mean ± SEM.

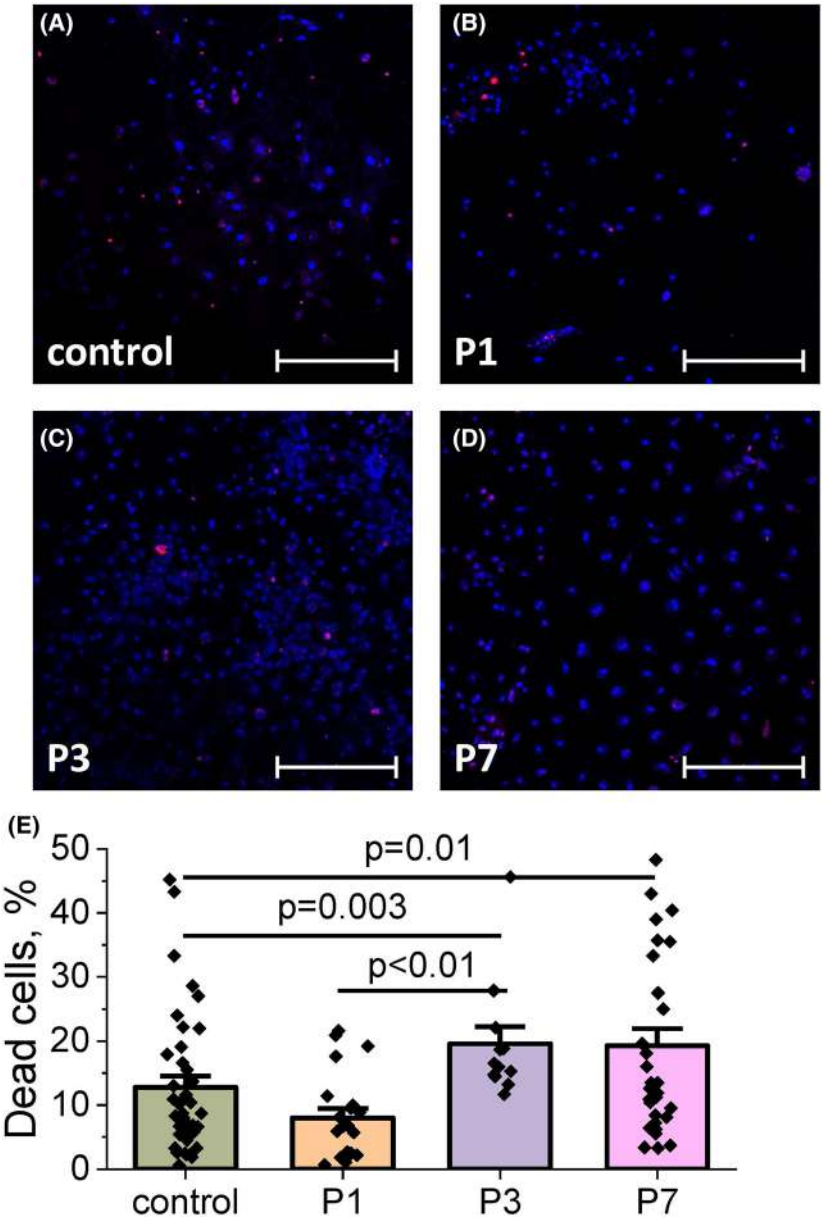

Fig. 6. RAGE activation protects brain cortex cells from cell death. Representative confocal images of Hoechst 33342- and PI-loaded cortical cells without pretreatment (A) (control) and after incubation with peptide P1 (B), P3 (C) and P7 (D) for 24 h. Scale bar = 200 μm. (E) The fraction of PI-positive cells normalized to the fraction of dead cells in the control group without peptide incubation. Data are presented as the mean ± SEM.

$N = 21$ fields of view). The results indicate no pathological consequences of ROS production activation by RAGE fragments.

Activation of RAGE by peptides (60–76) and Ac-(60–76)-NH_2 protects cells from βA-induced death

Significant acceleration of intracellular ROS production by NOX is one of the pathological processes leading to βA toxicity. A two-fold decrease ($P < 0.007$) of the βA-induced activation of HEt oxidation after cells incubation with FPS-ZM1 (Fig. 7A–C) indicates that βA toxicity is partly associated with binding of βA with RAGE. Incubation of primary co-cultures of cortical neurons and glial cells with βA and P1 leads to a statistically significant decrease in the PI-positive cells level compared to the experiment with βA only ($14.8 \pm 9.7\%$, $n = 3$ coverslips, $N = 21$ fields of view and $26.2 \pm 16.8\%$, $n = 3$ coverslips, $N = 58$ fields of view respectively) (Fig. 7D–F,I). Application of control P3 as well as P7 did not show a significant decrease in dead cells percentage ($19.5 \pm 2.8\%$, $n = 3$ coverslips, $N = 11$ fields of view and $32.6 \pm 16.7\%$, $n = 3$ coverslips, $N = 31$ fields of view respectively) (Fig. 7G–I).

Discussion

Dialogue about the possible regulation of NOX in brain cells by RAGE activation has been ongoing for a relatively long time considering the increase in ROS production in response to damage-associated and pathogen-associated molecules [22–24]. However, most of the damage-associated and pathogen-associated molecules able to activate RAGE are shown to be able to induce ROS in NOX through various mechanisms excluding RAGE, but, at the same time, inhibitors of this enzyme are protective in AGE-pathologies [8,25,26]. In the present study, we used short peptides from the RAGE V-domain that are unable to induce any cell death in primary co-cultures of neurons and astrocytes (Fig. 7). At the same time, these peptides stimulate RAGE-induced production of ROS in NOX. These results confirm that NOX in brain cells can be activated by RAGE and that ROS production from this enzyme plays role in redox signaling rather than induction of pathology and cell death.

Previously, we have shown that peptide 60–76 (P1) can induce RAGE-dependent activation of glutamate release from astrocytes that induced a calcium signal in neurons [4]. However, RAGE-induced activation of ROS was independent of glutamate antagonists (Fig. 4), although we cannot exclude the possible effect of ROS production on glutamate release in astrocytes.

Aβ is known to induce massive ROS production in NOX and this effect could be induced even with a nanomolar concentration of the oligomers [8,27]. The effects of peptide–RAGE-induced activation of NOX are much smaller compared to the effects of Aβ (Fig. 7). However, only peptides P1 and P7 that previously demonstrated the protective activity *in vivo* [15,16,18] were able to induce ROS production. It was also shown that fragments of the V-domain of RAGE protect neurons against Aβ induced apoptosis [17] and necrosis (Fig. 7). These protective effects could be induced by binding of peptide to Aβ and/or by direct binding of the peptide to RAGE.

Activation of the NOX through RAGE in our experiments lead to a decrease in GSH level and activation of lipid peroxidation that may be accepted as oxidative stress. However, this activation led to basal reduction in cell death and protection against Aβ cell death. The redox balance in the brain is significantly different between brain regions and neurons and astrocytes [21], which suggests different thresholds for the initiation of oxidative stress. Lipid peroxidation is essential for activation of phospholipase-dependent calcium signaling [28,29] and RAGE-induced activation of NOX and lipid peroxidation can be a part of the physiological signaling cascade including an effect on calcium stores [30].

The protective effect of the short peptide of RAGE is via binding with a possible RAGE agonist (including β-amyloid) and activation of RAGE following

Fig. 7. RAGE activation is protective against β-amyloid neurotoxicity. Aβ-induced ROS production activation (A) is reduced in the presence of RAGE antagonist (B) and does not change after pre-incubation of cells with peptide P1 (C). Each line corresponds to a single cell. Quantification of the Aβ influence on ROS production rate without additional exposure (control) and after pre-incubation of primary co-culture of cortical astrocytes and neurons with RAGE antagonist and peptide P1 (D). Representative confocal images of primary co-culture of cortical astrocytes and neurons loaded with Hoechst 33324 and PI without any additional exposure (E) and after preincubation with Aβ (F), a mixture of Aβ with P1 (G), Aβ with P3 (H), and Aβ with P7. Scale bar = 200 μm. (I) Quantification of the PI-positive cells fraction after different exposure conditions normalized to the fraction of dead cells in the control group without incubation. Data are presented as the mean ± SEM.

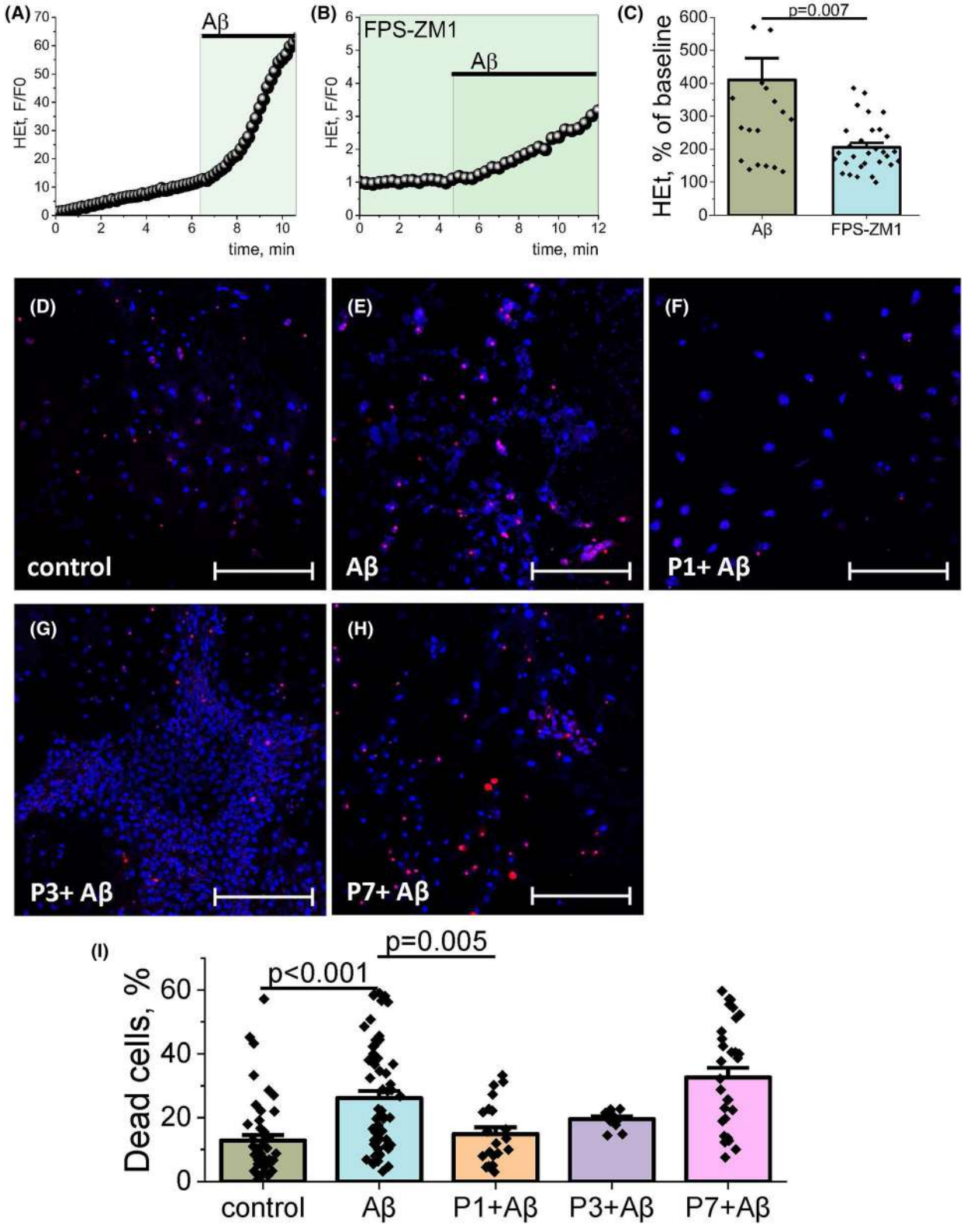
(A)
Aβ
HEt, F/F0
time, min
(B)
FPS-ZM1
Aβ
HEt, F/F0
time, min
(C)
p=0.007
HEt, % of baseline
Aβ
FPS-ZM1
(D)
control
(E)
Aβ
(F)
P1+ Aβ
(G)
P3+ Aβ
(H)
P7+ Aβ
(I)
p=0.005
p<0.001
Dead cells, %
control
Aβ
P1+Aβ
P3+Aβ
P7+Aβ

activation of a signaling cascade and NOX that is less likely accessed by application of full exogenous RAGE peptide.

Materials and methods

Synthetic peptides

RAGE fragments (Table 1) were derived from the sequences of human RAGE (Q15109 UniProtKB/Swiss-sProt). The RAGE peptides were synthesized by solid phase method as described previously [15,18].

Animals

For the experiments, 12-weeks male Wistar rats (250–300 g) and Wistar rat pups 2–4 days post-partum were used. Adult rats were housed with free access to water and food under a 12 : 12 h light/dark photocycle in an air-conditioned room at 22–24 °C. All of the animal procedures were performed in compliance with the ARRIVE guidelines and approved by the Institutional ethical committee of Orel State University (No. 18 dated 21.02.2020) in compliance with Russian Federation legislation.

Primary co-culture of neurons and preparation of glial cells

Co-cultures of cortical neurons and glial cells were isolated from pups as described previously [31] with modifications. After decapitation, the cortex was removed into an ice-cold Versene solution (Gibco, Waltham, MA, USA). The tissue was minced and trypsinized (Gibco) (0.05% for 15 min at 37 °C) and triturated. The mixed neurons and astrocytes suspension was plated onto polyethylenimine-coated 22 mm coverslips. Cells were maintained in Neurobasal A medium (Gibco) supplemented with B-27 (Gibco), 2 mM GlutaMax Supplement (Gibco) and 1% of penicillin/streptomycin. Cultures were maintained at 37 °C in a humidified atmosphere of 5% CO_2 and 95% air for a minimum of 12 days before experimental use. Neurons were easily distinguishable from glia: they appeared bright using phase contrast, had smooth rounded somata and distinct processes, and lay just above the focal plane of the glial layer.

Table 1. Amino acid sequences of the RAGE fragments.

Abbreviation	Number	Amino acid sequence
P1	60–76	AWKVLSPQGGGPWDSVA
P2	60–70	AWKVLSPQGGG
P3	60–62	AWK
P4	60–65	AWKVLS-G
P5	65–76	SPQGGGPWDSVA
P7	Ac-(60–76)-NH_2	Ac-AWKVLSPQGGGPWDSVA-NH_2

Cells were used at 12–16 days *in vitro*. The ratio of neurons : astrocytes was 60 : 40%.

Isolated cortical astrocytes were prepared as previously described [30]. Cerebra taken from 2–5-day-old Sprague–Dawley rats (University College London breeding colony). The cerebra were chopped and triturated until homogenous and trypsinized (50 000 $U{\cdot}mL^{-1}$ porcine pancreas; Sigma, St Louis, MO, USA) with 336 $U{\cdot}mL^{-1}$ DNAse 1 (bovine pancreas; Sigma) and collagenase 1.033 $U{\cdot}mL^{-1}$ (Sigma) at 37 °C for 15 min. After the addition of fetal bovine serum (10% of final volume) and filtering through 140-μM mesh, the tissue was centrifuged through 0.4 M sucrose (400 ***g*** for 10 min) and the resulting pellet transferred to Dulbecco's modified Eagle's medium supplemented with 5% fetal calf serum, 2 mM glutamine and 1 mM malate in tissue culture flasks pre-coated with 0.01% poly-D-lysine. The cells reached confluency at 12–14 days *in vitro*, and were harvested and reseeded onto 24-mm diameter glass coverslips, precoated with 0.01% poly-D-lysine for fluorescence measurements and used for 2–4 days.

Acute brain slices

Acute brain slices were prepared as described previously [32]. After rat decapitation, the brain was extracted and placed into an ice-cold Hanks' Balanced Salt Solution (HBSS) (Gibco) (pH 7.4 and 4 °C), followed sagittal section and preparation of cortical slices with a thickness of 300–500 μm. Slices were kept in an ice-cold HBSS with slight oxygenation. Before the experiments, slices were removed in HBSS (pH 7.4 and 37 °C) and stored for at least 1 h at 37 °C.

Live cell imaging

Fluorescence measurements were performed using a LSM 900 confocal microscope (Carl Zeiss Microscopy GmbH, Jena, Germany) and a 63× oil immersion objective.

Cytosolic ROS

HEt (5 μM) (Invitrogen, Carlsbad, CA, USA) was used for measurement of cytosolic ROS production in acute brain slices, as well in primary co-cultures of cortical neurons and glial cells. No preincubation ('loading') was used to limit the intracellular accumulation of oxidized products and HEt was presented in the solution during the experiment. The fluorescence of oxidized form of dihydroethidium was excited at 561 nm with detection above 575 nm.

Reduced GSH

Co-cultures of neurons and glial cells were incubated with 50 μM monochlorobimane (MCB) (Invitrogen) for 40 min

in HBSS prior to imaging. Then cells were washed with HBSS and images of the fluorescence of the MCB-GSH were acquired with excitation at 405 nm and emission at 435–485 nm.

Lipid peroxidation

For assessing lipid peroxidation, cells were loaded with 5 μM ratiometric probe C11-BODIPY 581/591 (Invitrogen) for 15 min and washed with HBSS. Excitatation at 488 and 561 nm and detection from 505 to 550 nm and above 580 nm were used for oxidized and reduced forms of the probe, respectively. Lipid peroxidation was calculated as the rate of increase of the 581/591 ratio.

Cell death

For measurement of necrotic cell death, co-cultures of neurons and glial cells were incubated with 5 μM Hoechst 33342 (Invitrogen) and 5 μM PI (Invitrogen) for 30 min at 37 °C, with subsequent washing with HBSS. Fluorescence of Hoechst 33342 and PI was excited at 405 and 561 nm with detection at 410–550 and 570–700 nm, respectively. Hoechst stains the total number of nuclei, whereas PI stains only cells with a disrupted plasma membrane. Dead cells (PI positive) were counted as a fraction of the total (Hoechst positive). In each experiment, 10 random fields were analyzed.

Statistical analysis

Data were analyzed with ORIGIN PRO 2018 (MicroCal, Northampton, MA, USA) and are presented as the mean ± SEM. A Mann–Whitney test was used to estimate statistical significance between experimental groups.

Acknowledgements

The present study was supported by a grant from the Russian Federation Government no. 075-15-2022-1095. Peptide synthesis and the experiments with the selective antagonist of RAGE were funded by the Russian Science Foundation, project number 23-74-00024.

Conflicts of interest

The authors declare that they have no conflicts of interest.

Author contributions

AYA, OMV, AYV, DOK and AVK designed the experiments. AYA, OMV and AYV supervised the design and course of the experiments. AYV, AVK, ESS and DOK performed the experiments. AYV, AYA, AVK and ESS performed the analyses and interpretation of the experiments. AYA, AYV and AVK wrote the manuscript. AYA, AYV, AVK, OMV, DOK and ESS reviewed and edited the manuscript. All of the authors read and approved the final version of the manuscript submitted for publication.

Data availability statement

The datasets used and/or analyzed during the present study are available from the corresponding author upon reasonable request.

References

1 Buckley S & Ehrhardt C (2010) The receptor for advanced glycation end products (RAGE) and the lung. *J Biomed Biotechnol* **2010**, 917108.
2 Ramasamy R, Vannucci S, Yan S, Herold K, Yan S & Schmidt A (2005) Advanced glycation end products and RAGE: a common thread in aging, diabetes, neurodegeneration, and inflammation. *Glycobiology* **15**, 16R–28R.
3 Kim J, Wan C, J O'carroll S, Shaikh S & Nicholson L (2012) The role of receptor for advanced glycation end products (RAGE) in neuronal differentiation. *J Neurosci Res* **90**, 1136–1147.
4 Kamynina A, Esteras N, Koroev D, Angelova P, Volpina O & Abramov A (2021) Activation of RAGE leads to the release of glutamate from astrocytes and stimulates calcium signal in neurons. *J Cell Physiol* **236**, 6496–6506.
5 Angelova P (2021) Sources and triggers of oxidative damage in neurodegeneration. *Free Radic Biol Med* **173**, 52–63.
6 Gandhi S & Abramov A (2012) Mechanism of oxidative stress in neurodegeneration. *Oxid Med Cell Longev* **2012**, 428010.
7 Abramov A, Jacobson J, Wientjes F, Hothersall J, Canevari L & Duchen M (2005) Expression and modulation of an NADPH oxidase in mammalian astrocytes. *J Neurosci* **25**, 9176–9184.
8 Abramov A, Canevari L & Duchen M (2004) β-Amyloid peptides induce mitochondrial dysfunction and oxidative stress in astrocytes and death of neurons through activation of NADPH oxidase. *J Neurosci* **24**, 565–575.
9 Vermot A, Petit-Härtlein I, Smith S & Fieschi F (2021) Nadph oxidases (Nox): an overview from discovery, molecular mechanisms to physiology and pathology. *Antioxidants* **10**, 890.
10 Piras S, Furfaro A, Domenicotti C, Traverso N, Marinari U, Pronzato M & Nitti M (2016) RAGE

expression and ROS generation in neurons: differentiation versus damage. *Oxid Med Cell Longev* **2016**, 9348651.
11 Sangle G, Zhao R, Mizuno T & Shen G (2010) Involvement of RAGE, NADPH oxidase, and Ras/Raf-1 pathway in glycated LDL-induced expression of heat shock factor-1 and plasminogen activator inhibitor-1 in vascular endothelial cells. *Endocrinology* **151**, 4455–4466.
12 Borchi E, Bargelli V, Guidotti V, Berti A, Stefani M, Nediani C & Rigacci S (2014) Mild exposure of RIN-5F β-cells to human islet amyloid polypeptide aggregates upregulates antioxidant enzymes via NADPH oxidase-RAGE: an hormetic stimulus. *Redox Biol* **2**, 114–122.
13 Kay A, Simpson C & Stewart J (2016) The role of AGE/RAGE signaling in diabetes-mediated vascular calcification. *J Diabetes Res* **2016**, 6809703.
14 Lin C, Huang P, Chen C, Wu M, Chen J, Chen J & Lin S (2021) Sitagliptin attenuates arterial calcification by downregulating oxidative stress-induced receptor for advanced glycation end products in LDLR knockout mice. *Sci Rep* **11**, 1–14.
15 Volpina O, Samokhin A, Koroev D, Nesterova I, Volkova T, Medvinskaya N, Nekrasov P, Tatarnikova O, Kamynina A, Balasanyants S *et al.* (2018) Synthetic fragment of receptor for advanced glycation end products prevents memory loss and protects brain neurons in olfactory bulbectomized mice. *J Alzheimers Dis* **61**, 1061–1076.
16 Koroev D, Volpina O, Volkova T, Kamynina A, Samokhin A, Filatova M & Bobkova N (2019) A synthetic fragment of the receptor for glycation end products and its analogue improve memory in transgenic Alzheimer's disease mouse model. *Russ J Bioorg Chem* **45**, 361–365.
17 Kamynina A, Esteras N, Koroev D, Bobkova N, Balasanyants S, Simonyan R, Avetisyan A, Abramov A & Volpina O (2018) Synthetic fragments of receptor for advanced glycation end products bind beta-amyloid 1–40 and protect primary brain cells from beta-amyloid toxicity. *Front Neurosci* **12**, 1–9.
18 Volpina O, Koroev D, Serebryakova M, Volkova T, Kamynina A & Bobkova N (2021) Proteolytic degradation patterns of the receptor for advanced glycation end products peptide fragments correlate with their neuroprotective activity in Alzheimer's disease models. *Drug Dev Res* **82**, 1217–1226.
19 Cho S, Wood A & Bowlby M (2007) Brain slices as models for neurodegenerative disease and screening platforms to identify novel therapeutics. *Curr Neuropharmacol* **5**, 19–33.
20 Domijan A-M, Kovac S & Abramov A (2014) Lipid peroxidation is essential for phospholipase C activity and the inositol-trisphosphate-related Ca(2)(+) signal. *J Cell Sci* **127**, 21–26.
21 Vinokurov A, Stelmashuk O, Ukolova P, Zherebtsov E & Abramov A (2021) Brain region specificity in reactive oxygen species production and maintenance of redox balance. *Free Radic Biol Med* **174**, 195–201.
22 Yan S, Chen X, Fu J, Chen M, Zhu H, Roher A, Slattery T, Zhao L, Nagashima M, Morser J *et al.* (1996) RAGE and amyloid-beta peptide neurotoxicity in Alzheimer's disease. *Nature* **382**, 685–691.
23 Wautier M, Chappey O, Corda S, Stern D, Schmidt A & Wautier J (2001) Activation of NADPH oxidase by AGE links oxidant stress to altered gene expression via RAGE. *Am J Physiol Endocrinol Metab* **280**, E685–E694.
24 Carrano A, Hoozemans J, van der Vies S, Rozemuller A, van Horssen J & de Vries H (2011) Amyloid beta induces oxidative stress-mediated blood–brain barrier changes in capillary amyloid angiopathy. *Antioxid Redox Signal* **15**, 1167–1178.
25 Abramov A, Ionov M, Pavlov E & Duchen M (2011) Membrane cholesterol content plays a key role in the neurotoxicity of β-amyloid: implications for Alzheimer's disease. *Aging Cell* **10**, 595–603.
26 Thallas-Bonke V, Thorpe S, Coughlan M, Fukami K, Yap F, Sourris K, Penfold S, Bach L, Cooper M & Forbes J (2008) Inhibition of NADPH oxidase prevents advanced glycation end product-mediated damage in diabetic nephropathy through a protein kinase C-α-dependent pathway. *Diabetes* **57**, 460–469.
27 Narayan P, Holmström K, Kim D, Whitcomb D, Wilson M, St. George-Hyslop P, Wood N, Dobson C, Cho K, Abramov A *et al.* (2014) Rare individual amyloid-β oligomers act on astrocytes to initiate neuronal damage. *Biochemistry* **53**, 2442–2453.
28 Vaarmann A, Gandhi S & Abramov A (2010) Dopamine induces Ca2+ signaling in astrocytes through reactive oxygen species generated by monoamine oxidase. *J Biol Chem* **285**, 25018–25023.
29 Novikova I, Manole A, Zherebtsov E, Stavtsev D, Vukolova M, Dunaev A, Angelova P & Abramov A (2020) Adrenaline induces calcium signal in astrocytes and vasoconstriction via activation of monoamine oxidase. *Free Radic Biol Med* **159**, 15–22.
30 Gola L, Bierhansl L, Csatári J, Schroeter C, Korn L, Narayanan V, Cerina M, Abdolahi S, Speicher A, Hermann A *et al.* (2023) NOX4-derived ROS are neuroprotective by balancing intracellular calcium stores. *Cell Mol Life Sci* **80**, 127.
31 Esteras N, Blacker T, Zherebtsov E, Stelmashchuk O, Zhang Y, Wigley W, Duchen M, Dinkova-Kostova A & Abramov A (2023) Nrf2 regulates glucose uptake and metabolism in neurons and astrocytes. *Redox Biol* **62**, 102672.
32 Vinokurov A, Dremin V, Piavchenko G, Stelmashchuk O, Angelova P & Abramov A (2021) Assessment of mitochondrial membrane potential and NADH redox state in acute brain slices. *Methods Mol Biol* **2276**, 193–202.